Sensors & Diagnostics

CRITICAL REVIEW

View Article Online
View Journal | View Issue



Cite this: *Sens. Diagn.*, 2023, **2**, 781

# Recent advances of peroxidase-active nanozymes in electrochemical immunoassays

Jiejie Feng, Tao Yao and Zhanfang Ma *

A new type of nanomaterial with peroxidase activity (peroxidase-active nanozyme) has been widely used in the design of electrochemical immunosensors. Due to the high and tunable catalytic activity, ease of modification, large surface area, and low cost, they have gradually emerged as alternatives to natural enzymes. To date, a variety of peroxidase-active nanozymes have been reported, including metal–organic frameworks (MOFs), transition metal-based oxygenated compounds (oxides, peroxides, and hydroxides), noble metal nanoparticles, Prussian blue and other transition metal-containing biomolecules, which have been successfully applied to the construction of electrochemical immunoprobes and substrates. Herein, we briefly summarize the research progress on peroxidase-active nanozymes that have been successfully applied to electrochemical immunosensors in recent years, including their synthesis, the assembly steps of the constructed sensors, and the working mechanism. We also discuss some problems encountered in the application of these nanozymes in electrochemical immunosensors and provide some possible strategies to address these limitations. We hope that this review will be helpful for researchers to understand and select such nanozymes, and it will also promote the development of novel electrochemical immunosensors with excellent performance in the future.

Received 20th March 2023,
Accepted 25th April 2023

DOI: 10.1039/d3sd00061c

rsc.li/sensors



## 1. Introduction

In the context of today's severe pandemic, the early diagnosis of disease is conducive to subsequent treatment and rehabilitation.[1–3] During the early stages of morbidity, the content of some proteins or metabolites, namely disease markers, closely related to the disease categories fluctuates markedly beyond the range of normal values.[4–6] Hence, precise monitoring for these biomarkers has become pivotal in preventing the deterioration of disease.[7–9] Recently, a variety of detection methods, including electrochemical immunoassay,[10–12] mass spectrometry immunoassay,[13] fluorescence immunoassay,[14] and electrochemiluminescence immunoassay,[15] have been widely developed for the accurate detection of disease markers. The electrochemical technique, in particular, has attracted considerable interest owing to its advantages, such as wide dynamic range, facile operation, high specificity, prominent sensitivity, and easy miniaturization.[16–20]

Regarding the composition of electrochemical immunosensors, there are three integrated components that

*Department of Chemistry, Capital Normal University, Beijing 100048, China.*
*E-mail: mazhanfang@cnu.edu.cn*

**Jiejie Feng**

*Jiejie Feng received his B.E. degree from Shandong Agricultural University in 2018. He is currently a graduate student at Capital Normal University. His research is focused on electrochemical immunosensors and the synthesis of nanomaterials.*

**Tao Yao**

*Tao Yao received his B.E. degree from Shihezi University in 2019. He is currently a graduate student at Capital Normal University. His research is focused on nanofabrication and electrochemical immunosensors.*

are needed to be considered in the designing strategy: i) the modification of the biorecognition elements, including aptamers, antibodies, and peptides, is an essential step in designing the immunosensing interface, which can directly affect their specific interactions with the targets. ii) Signal transducers as the central elements can produce measurable signals based on the content of the target. This component can determine the quality of the biosensor directly, and the straightforward influences are related to the sensitivity, selectivity, and stability of sensors. iii) Electronic data management system is the final elements to achieve the readout of electrochemical signals, including electron transfer resistance, surface conductivity, and redox reaction potential/current.[21,22] Considering the key action of signal transduction, various strategies have been proposed to improve the readout of electrochemical signals, for instance, the introduction of catalytic amplification tactics.[23,24] Enzymes, as powerful catalysts, are always introduced into the design of catalytic reaction-based immunoassays.[25,26] Enzymes certainly play an important role in electrochemical immunosensors, and enzyme-induced catalytic reactions to amplify the readout signal have become a common method to improve the sensitivity of immunosensors. However, the extraction and storage of biological enzymes require strict and demanding conditions, and their activity is also greatly affected by the environment. Therefore, on this basis, nanozymes are developed to solve this situation.[27]

Nanoenzymes are a class of nanomaterials with enzyme-mimicking activity, which have aroused great interest from researchers in designing electrochemical immunosensing interfaces.[28,29] Since they were first proposed to describe the ribonuclease-like activity of gold nanoparticles, various functional materials with nanoscale sizes have been found to have other enzyme-like properties, such as glucose oxidase, sulfite oxidase, superoxide dismutase, and peroxidase. Like with enzymes, temperature is an important factor that can influence nanozyme activity. Most nanomaterials exhibit nanozyme activity at temperatures above 35 °C, however, there are several nanozymes reported in recent times that show superior nanozyme activity at room temperature.[110–112]

**Zhanfang Ma**

*Zhanfang Ma received his PhD in Colloid and Interface Science at the Key Laboratory of Colloid and Interface Science, Institute of Photographic Chemistry, Chinese Academy of Sciences. He is currently a full professor of physical chemistry in the Department of Chemistry at Capital Normal University. His current research interests include nanobiosensors, nanofabrication, and electrochemical biosensors.*

Among all the discovered artificial enzymes, the peroxidase family is one of the most commonly found and is mainly divided into three categories including peroxidase, glutathione peroxidase, and halo peroxidase.[30] For their catalytic reaction, a radical mechanism was verified by researchers and it mainly depends on the exposed active sites for the different nanozymes.[31] For instance, numerous carbon-based nanozymes have been found to exhibit excellent peroxidase-like activity due to their –C═O and –O ═CO– groups; this is different from the ping-pong reaction mechanism for $Fe_3O_4$. Hence, before exploring the catalytic mechanism, it is necessary to have a clear understanding of the structure of nanozymes. Depending on the composition, the reported nanozymes are mainly divided into nanomaterials containing metal active sites (like MOFs, metallic oxides, and noble metals) and carbon-based nanomaterials with different dimensions (like graphene, carbon nanotubes, and g-$C_3N_4$). In comparison to natural peroxidases, nanozymes have many remarkable advantages when they are applied in designing electrochemical immunosensors as follows. i) High and tuneable catalytic activities.[32,33] Compared with the fixed molecular structure of natural enzymes, the catalytic activity of most peroxidases can be optimized to a more ideal level by changing the components added during their synthesis. ii) Ease of modification.[34] Nanozymes often contain some functional groups like carboxyl, amino, and hydroxyl groups in their structure, which can be chemically conjugated with biomolecules including antibodies and nucleic acids when participating in the construction of electrochemical sensing interfaces without the need for complex pre-treatment. Physical methods like electrostatic interaction are also used for the modification of nanozymes. iii) Large specific surface area.[35] The large specific surface area of nanozymes usually means the exposure of more catalytic active sites, and it is also beneficial to improve the mass transfer efficiency of the substrate solution molecules in the catalyst for a thorough catalytic reaction. iv) Low cost and large-scale production.[36] Different from the limitations of high cost and harsh reaction conditions of natural enzymes, cheap raw materials, simple synthesis steps, and mild reaction conditions allow nanoenzymes to better help electrochemical sensors towards practical application. With these merits, nanozymes with peroxidase-like activity have been widely applied in constructing electrochemical immunosensors. As such, we have overviewed some peroxidase-active nanozyme-based electrochemical immunosensors.

This review describes the recent progress on electrochemical immunosensors based on the peroxidase-active nanozymes for detecting various disease markers. The nanostructure of these nanozymes and the working mechanisms of sensors are discussed, along with the challenges of these nanozymes in constructing immunosensing interfaces. This review provides a comprehensive understanding and new insight for the design of advanced biosensors.

## 2. Type of peroxidase-active nanozymes

Research on the applications of peroxidases in designing electrochemical immunosensors is constant since nanomaterials with peroxidase-like catalytic behaviour have been developed through indefatigable exploration. For the catalytic mechanism of nanozymes in peroxidase-mimicking reactions, the hydroxyl radical generation path based on the Fenton reaction and the electron transfer path are two of the most typical approaches.[37] Some nanozymes with peroxidase-like activity, especially the iron-based nanomaterials, can efficaciously decompose $H_2O_2$ into hydroxyl radicals and further react with the redox substrate, and a Fenton reaction can be immediately induced during this process. Besides, for some kinds of nanozymes, such as cobalt-based nanomaterials, their peroxidase-like activity does not originate from the Fenton reaction with a ceaselessly expanding and deepening scope. In this regard, the substrate can be oxidized directly on account of an electron transfer from lone-pair electrons to the nanozymes (as an electron acceptor to be reduced) and $H_2O_2$ subsequently receives electrons from nanozymes (as an electron donor to be oxidized) to decompose and generate $^{\cdot}OH$.[38] However, regardless of the catalytic path, the peroxidase-like activity of these nanozymes can all be authenticated with some chromophores like 3,3,5,5-tetramethylbenzidine (TMB) and is mostly used for signal amplification when they are adopted in the construction of electrochemical immunosensors. Herein, we present several common peroxidase-active nanozymes as follows.

### 2.1 Noble metal nanoparticles

Due to their desirable optical and electronic properties, large specific surface area, stability, and enzyme-like catalytic activity, noble metal nanoparticles often serve as remarkable candidates for designing immunoprobes and substrates.[39–43] Traditional noble metals mainly include gold, silver, platinum, ruthenium, rhodium, iridium, and palladium. When these noble metal nanoparticles participate in the construction of immunosensing interfaces, on the one hand, they can be directly combined with biological molecules (such as antibodies, nucleic acids, and peptides), small organic molecules, and other materials (such as MOFs, graphene and carbon nanotubes) alone. On the other hand, alloys formed by two or more noble metals tend to have better enzyme-like catalytic effects and electrical conductivity. As one of the most commonly used nanomaterials, many related electrochemical immunosensors that have remarkable analytical performance have been reported.[44–47]

Liu and co-workers have proposed a multifunctional nanoprobe-based β-cyclodextrin-embellished graphene nanosheet. To achieve high peroxidase-like activity, the ternary hollow Pt/PdCu nanocubes were subsequently reduced on the three-dimensional graphene framework and further served as the anchor to fix antibodies through Pd–$NH_2$ and Pt–$NH_2$, which exhibited extraordinary peroxidase-like activity towards $H_2O_2$. Under the optimal conditions, the as-designed immunosensor, which is applicable for the quantitative detection of SCCA, displayed a low detection limit with a broad linear range, good sensitivity, and reproducibility (Fig. 1).[48]

Noble metal nanoparticles have excellent peroxide-like activity and simple preparation but they are often limited by the high cost of raw material. Therefore, it is necessary to develop non-noble metal enzyme-like catalysts.

### 2.2 Metal–organic frameworks

MOFs are outstanding materials for fabricating sensing platforms because they have lots of excellent functionalities including their admirable adsorption capacity, adjustable morphological structure, high specific surface area, and some even have remarkable enzyme-like activity. They are porous crystalline materials and have generally been assembled by metal nodes (zinc ions, cobalt ions, ferric ions, copper ions, and zirconium ions, *etc.*) and organic ligands (methylimidazole, terephthalic acid, and nitrilotribenzoic acid, *etc.*) *via* coordination bonding, which fundamentally determine their intrinsic features. Due to their versatility and flexible synthetic design, an increasing number of pristine MOFs, MOF composites, and MOF derivatives have been widely applied in constructing electrochemical immunosensing interfaces, especially for the preparation of bioprobes and substrate composites.[49–53] Among all the reported MOFs, Fe-MOFs have been widely used in the design of electrochemical immunosensors due to their remarkable peroxidase activity and satisfactory acid–base tolerance.[54–57]

Originally, inspired by the composition of the peroxidase-employed iron porphyrin as the catalytical cofactor, myriad

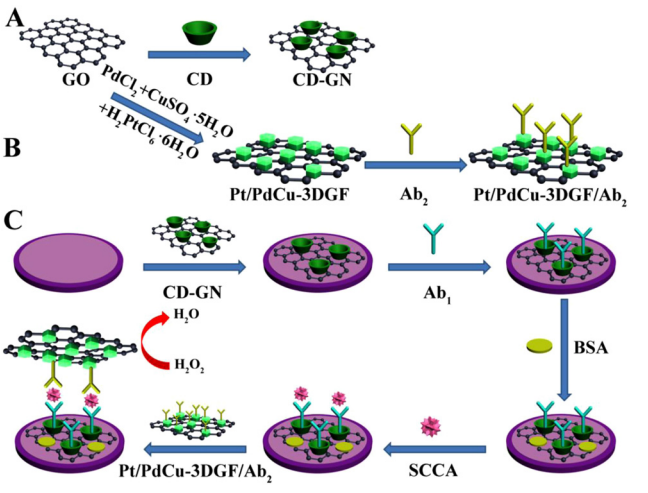


Fig. 1 Schematic illustration of the construction of electrochemical immunosensors based on Pt/PdCu nanocubes-modified β-cyclodextrin/graphene oxide (reprinted with permission from ref. 48, copyright 2016 Elsevier).

sagacious designs have focused on the exploitation of MOFs with peroxidase-like activity because the iron and porphyrin can be excellent candidates for the central metal ions and ligands, respectively. Hence, nanozymes based on Fe-MOFs are simply divided into two kinds, including central iron ion-dominated and iron porphyrin ligand-dominated MOFs. For the former, Fe-MIL-$NH_2$-88B coordinated with ferric ions and 2-aminoterephthalic acid ($NH_2$-BDC) is a pervasive Fe-MOF with peroxidase-like activity in the application of electrochemical immunosensors since it was first discovered. With abundant amino groups and uniform internal orifices in its regular octahedra, Fe-MIL-88B-$NH_2$ can be commendably embellished with biomolecules and improve the catalytic efficiency for $H_2O_2$. Recently, a hemin@Fe-MIL-88$NH_2$/AuPt composite was prepared as a bioprobe to improve the responsive current with a cascade amplification strategy. Synergistic catalytic effects of hemin, MOFs, AuPt and HRP allow this immunosensor to achieve a wide detection range of 0.1–50 ng $mL^{-1}$ and a low detection limit of 0.045 ng $mL^{-1}$ through an indirect competitive format for the analysis of maduramicin (MD).[58] The successful assembly of the immunosensor was also verified by electrochemical impedance spectroscopy (EIS) and cyclic voltammetry (CV). Apart from the aforementioned application, Fe-MIL-$NH_2$-88B has served as the support for deposit gold nanoparticles (Au NPs) and was ulteriorly immobilized on N-doped graphene nanoribbons to form an immune-substrate. Notably, Au NPs can be efficaciously mounted on the surface of Fe-MOFs only with the *in situ* reduction of $HAuCl_4$. Such an immune-substrate not only provides active sites for the fixation of primary antibodies but also accelerates the electron transfer rate to improve the sensitivity of this immunosensor.[59]

Another reported Fe-MOF that has been introduced in electrochemical immunosensor is $NH_2$-MIL-53 (Fe). Similar to the morphology of $NH_2$-MIL-88B, $NH_2$-MIL-53, with a spindle shape (~1.0 μm in length and ~0.5 μm in width), always has a smooth surface and rich amino groups on its surface can also facilely implement many post-modification steps during the assembly of the sensor element. Luo and co-workers employed $NH_2$-MIL-53 as a signal amplifier to be integrated with PdPt NPs to obtain an immunoprobe of high electrocatalytic activity for $H_2O_2$. With several controlled experiments, it was shown that the distinguished catalytic ability was mainly ascribed to PdPt NPs and displayed excellent analytical performance for prolactin (Fig. 2).[60]

Some copper-based MOFs with peroxidase-like activity have been reported as well, and most of them for the catalysis of $H_2O_2$ mainly benefit from the transformation between copper(II) and copper(I). Because of this, copper-based MOFs are widely applied in electrochemical immunosensors.[61–63] Through the development of other Cu-based compounds with intrinsic peroxidase-like activities, many Cu-MOF nanozymes have been prepared along with the design of various organic ligands to coordinate with copper ions since the catalysis of a Cu-MOF named HKUST-1 was confirmed in the presence of $H_2O_2$. 1,3,5-Benzenetricarboxylic

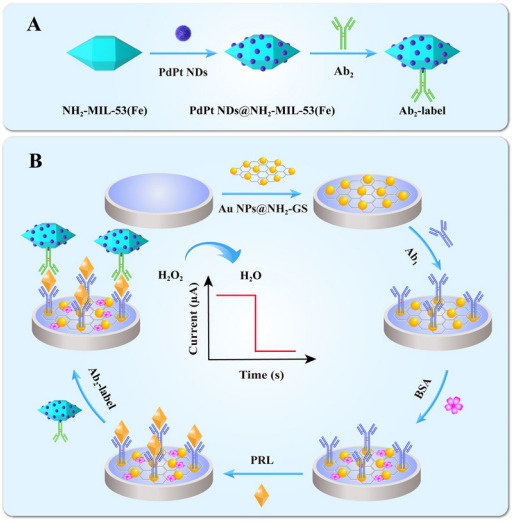


Fig. 2 (A) Representation of $Ab_2$–PdPt NDs@$NH_2$-MIL-53(Fe). (B) Fabrication of an electrochemical immunosensor (reprinted with permission from ref. 60, copyright 2021 Elsevier).

acid (BTC) and $NH_2$-BDC, as the common organic ligands, easily synthesize the Cu-MOFs and further combine with biomolecules so that selective recognition can be achieved. Zhang and co-workers proposed an efficient signal amplification strategy based on a novel Cu-MOFs immunoprobe-participating radical polymerization and constructed an impedimetric immunosensor for the detection of CA15-3. As shown in Fig. 3(1), with the self-carried amino anchor, CA15-3 antibody and glucose oxidase can be combined with the surface of the Cu-MOFs sphere to form an immunoprobe through a Schiff base reaction and was characterized by Fourier transform infrared spectroscopy (FT-IR) (Fig. 3(2)). As expected, a cascade reaction was

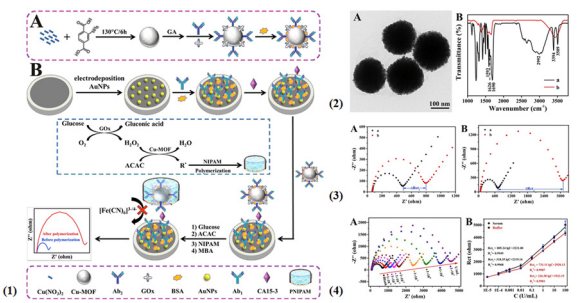


Fig. 3 (1) The preparation process of immunoprobes (A) and a schematic illustration of cascade catalysis-initiated radical polymerization-triggered signal amplification for the electrochemical detection of CA15-3 (B). (2) TEM image of Cu-MOFs (A) and FTIR spectra (B) of $NH_2$–$H_2$BDC (a), and Cu-MOFs (b). (3) The contrast in the EIS resistance values in 5 mM $[Fe(CN)_6]^{3-/4-}$ containing 0.1 M KCl: the immunosensor without (A) and with (B) radical polymerization amplification. The immunosensor was incubated without 1 U $mL^{-1}$ CA15-3 (a) and with CA15-3 (b). (4) (A) EIS response of the electrochemical biosensor and (B) the calibration curve of resistance values for target CA15-3 from blank to 100 U $mL^{-1}$ in buffer (reprinted with permission from ref. 64, copyright 2019 Elsevier).

triggered once the oxidization of glucose was catalysed by glucose oxidase to generate $H_2O_2$ and many acetylacetone radicals were subsequently yielded with the catalysis of Cu-MOFs. Through the verification of the controlled group (with and without the incubation of CA15-3 antigen), the $\Delta R_{ct}$ value after radical polymerization was higher ($\Delta R_{ct2}$ = 2292.9 Ω) than that before radical polymerization ($\Delta R_{ct1}$ = 302.3 Ω), providing the feasibility of this signal amplification strategy (Fig. 3(3)) and achieving the quantitative detection of CA 15-3 (Fig. 3(4)).[64] Apart from the aforementioned Cu-MOFs, $Cu_3(BTC)_2$ composed of copper ions, and BTC was designed as another bioprobe for $H_2O_2$.

However, $Cu_3(BTC)_2$ always requires non-native mediated materials like noble metal particles to concatenate biomolecules with covalent bonding. Li *et al.* reported that a $Cu_2O@Cu_3(BTC)_2$ core–shell structure was adopted in the design of immunoprobes and in order to couple with biomolecules (antibody and horseradish peroxidase (HRP)), chloroauric acid was reduced on the surface of $Cu_3(BTC)_2$ to form $Cu_2O@Cu_3(BTC)_2@Au$. The synergistic effect of $Cu_2O$, $Cu_3(BTC)_2$, and HRP efficaciously promoted the reduction of hydrogen peroxide and tripled the amplification of electrical signals for the detection of CEA.[65]

Co-MOFs are a class of crystalline porous organic–inorganic hybrid materials formed *via* auto-assemblage between Co ions and appropriate organic ligands like methylimidazole, and 1,4-benzenedicarboxylate. Different coordination surroundings between the cobalt ions and diverse organic ligands directly determine the characteristics of Co-MOFs.[66–70] Among all the Co-MOFs, ZIF-67, which is composed of $Co^{2+}$ and 2-methlyimidazole, has received widespread attention in various fields like catalysis and sensors. ZIF-67 has a cubic crystal symmetry with unit cell parameters $a = b = c$ = 16.9589 Å, and exhibits a high surface area ($S_{BET} > 1700\ m^2\ g^{-1}$) that endows it with abundant active sites. Meanwhile, the presence of micropores of 0.34 nm is favourable for chemical reactions due to their strong affinity for solution molecules. With the characteristics of highly stable structure, tunable pore aperture, and easy preparation, ZIF-67 and its derivatives have received widespread research interest for designing electrochemical immunosensors.[71–74] For example, Dai and co-workers prepared a sandwich-type immunosensor for prostate-specific antigen detection based on a ZIF-67 immunoprobe. At room temperature, hexadecimal ZIF-67 was successfully prepared and further embellished with Pd NPs by the *in situ* reduction of $H_2PdCl_4$ (Fig. 4). Similar to Fe-MOFs and Cu-MOFs, Co-MOFs exhibited excellent peroxidase-like activity and created a synergistic effect with Pd NPs to obtain further signal amplification. Based on this simple assembly strategy, this immunosensor showed a wide detection range of 0.00001–50 ng $mL^{-1}$ and a low detection limit of 0.03 pg $mL^{-1}$.[75]

Besides the catalytic properties of Co-MOFs, there are also studies that combine them with other conductive materials to alter the electronic structure. Another type of Co-MOF, synthesized by $Co^{2+}$ and benzene-1,3,5-tricarboxylate (Co–BTC), was used to mix the graphene oxide to form a substrate matrix by a one-step hydrothermal method. With the help of graphene oxide, Co–BTC had excellent dispersibility and its electronic conductivity was also clearly improved. Based on Co–BTC/GO composites, the resulting immunosensor showed high responsiveness, and selectivity in detecting a real-time serum sample.[76]

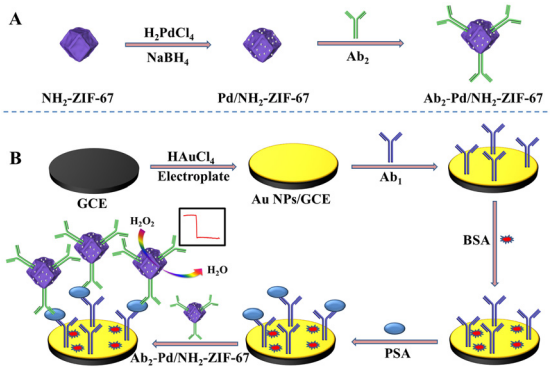


**Fig. 4** A schematic showing the preparation of the electrochemical immunosensing interface based on ZIF-67 (reprinted with permission from ref. 75, copyright 2019 Elsevier).

As a kind of nanomaterial, MOFs have good designability. By adjusting the type of ligand and metal ions, MOFs can be endowed with different physicochemical properties. However, poor conductivity and dispersibility in water are always important factors that restrict them in constructing electrochemical immunosensing interfaces.

### 2.3 Metal-based oxygenated compounds

The intrinsic peroxidase-mimicking properties of $Fe_3O_4$ magnetic NPs are always available for hydrogen peroxide catalysis due to their accessibility, and excellent catalytic activity, and have gradually evolved as the succedaneums for natural enzymes since they were first discovered by Yan's group in 2007. A ping-pong catalytic mechanism of $Fe_3O_4$ nanozymes was suggested through the kinetics studies for chromogenic reactions and thus widely adopted in the application of biosensors. With the restriction of a natural peroxidase-like external environment (pH and temperature) and difficult purification, more of them also found application in the electrochemical detection of tumor markers. The Hong group reported a new signal probe composed of ferroferric oxide@silica-amino groups ($Fe_3O_4@SiO_2–NH_2$) to hasten the decomposition of $H_2O_2$ to further accelerate the electron transfer of carboxylated ferrocene (Fc-COOH) on the electrode interface so that they obtained an acceptable $K_s$ value of 0.3967 $s^{-1}$ for Fc, indicating that a fast electron transfer kinetics process can be achieved to amplify signals.[77] Under the optimized conditions, this immunoassay showed excellent analytical performance, including a wide dynamic response range from 0.001 to 80 ng $mL^{-1}$ and a relatively low detection limit of 0.2 pg $mL^{-1}$ for carcinoembryonic antigen (CEA). $Fe_3O_4$ also

combines with some other nanozymes with peroxidase-like activity to achieve synergistic catalysis. A dumbbell-like Au–$Fe_3O_4$ nanoparticle was used as an immunoprobe to effectively accelerate the catalysis of $H_2O_2$ with the synergistic effect between Au and $Fe_3O_4$, proving that the effect of signal amplification made by Au–$Fe_3O_4$ is more obvious than any one of them.[78] $Fe_2O_3$ as another iron-based oxygenated compound is also reported to have peroxide-like activity. One typical sample is mesoporous $Fe_2O_3$ with peroxidase mimetic activity, which was successfully synthesized by the Bhattacharjee group, and directly applied in the detection of global DNA methylation, achieving excellent analytical performance.[79] Besides the intrinsic peroxide-like activity, this partner of Au–$Fe_2O_3$ always serves as carrier to fix biomolecules. For example, a gold-loaded nanoporous iron oxide nanocube (Au@NP$Fe_2O_3$NC) was embellished with p53 autoantibodies to be 'dispersible nanocapture agents' in serum samples, which can sensitively capture the target antigen to achieve a two-channel detection including electrochemical and naked-eyed readout modes.[80]

Iron-based hydroxides are also well-known peroxidase-like catalysts that are mostly prepared through a sacrificial template method, and typically incorporated with a compatible support to participate in the design of immunoprobes. A recent study on $Fe(OH)_3$ nanocages was proposed to construct the immunosensing interface for the sensitive detection of carbohydrate antigen 19-9 (CA 19-9). In the search for immobilization supports, gold-reduced graphene oxide (Au–rGO) was employed as the matrix material to affix the $Fe(OH)_3$ nanocage as well as the labelling antibody *via* electrostatic interactions and covalent coupling, respectively. With the assistance of numerous coordinated ferric ions in nanocages, methylene blue (MB) was used as a signal molecule covered with Au–rGO and was degraded while $H_2O_2$ was incubated on the electrode surface in which a Fenton reaction was promptly started to produce hydroxyl radicals; the responsive current was accordingly decreased to indicate the content of CA 19-9 (Fig. 5). Since it is an ionic compound with an incompact surface, molecule accessibility endowed it with excellent analytical performance including a wide linear range from 0.00001 to 100 U $mL^{-1}$ and an ultra-low detection limit of 0.785 U $mL^{-1}$.[81]

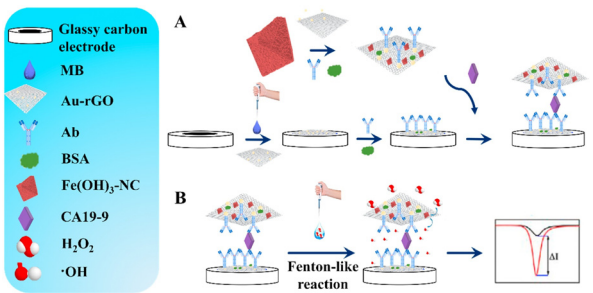


Fig. 5 Schematic illustration of the electrochemical immunosensor for CA19-9 (reprinted with permission from ref. 81, copyright 2021 Elsevier).

Besides the representative iron-based oxygenated compounds mentioned above, other copper-based nanozymes including cuprous oxide, cuprous peroxide and copper hydroxide have also been reported to have peroxidase-like activity.[82–84] Li and co-workers have proposed a novel immunoprobe with excellent catalytic activity towards $H_2O_2$, which adopted cuprous oxidase as the framework and modified it with titanium dioxide and platinum–copper nanoparticles in sequence. Meanwhile, $MoS_2$ loaded with gold nanoparticles was also prepared for the substrate. The resultant nanocomposite (cuprous oxide decorated with titanium dioxide octahedra-loaded dendritic platinum–copper nanoparticles) demonstrated uniform octahedral morphology and size, which effectively increased the catalytically active sites and specific surface area to load the secondary antibody.[85]

Apart from the aforementioned oxygenated compounds, ZIF-8-coated cuprous peroxide nanoparticles were successfully fabricated by our group using a one-step synthesis method. The nanoparticles can be used as probes to release copper ions in the case of acid hydrolysis and rapidly mix with hydrogen peroxide to trigger the Fenton reaction. At the same time, a large number of hydroxyl radicals were generated to degrade the polymer already fixed on the substrate, completing the change of the electrochemical signal. By this cascade amplification strategy, this proposed electrochemical immunosensor achieved excellent analytical performance towards CA-199 and showed good stability, selectivity, and repeatability.[86]

Besides the iron and copper-based peroxidase-active nanozymes, $Co_3O_4$ as a traditional metal oxide has been widely exploited in biosensors, supercapacitors, drug delivery, lithium-ion batteries, solar energy absorbers, gas sensing and so on.[87–91] Regarding their in-depth studies, the earliest report of their intrinsic peroxidase-like activity was made by Mu *et al.* and a relevant mechanism toward the catalysis to $H_2O_2$ was also given in terms of a series of steady-state kinetic experiments. Similar to the traditional Horseradish peroxidase (HRP), the catalytic activity of $Co_3O_4$ is also dependent on pH, temperature and substrate concentration. Its catalytic activity is much higher in weakly acidic solutions than in natural or basic conditions, and the optimal catalytic temperature is about 45 °C, ranging between 25 °C to 65 °C. Besides, unlike HRP, excess $H_2O_2$ cannot inhibit the catalytic activity of $Co_3O_4$ through conversion to inactive forms. The concrete catalytic mechanism of $Co_3O_4$ towards $H_2O_2$ is as follows.[92,93]

$$H_2O_2 + OH^- \leftrightarrow OOH^- + H_2O$$

$$Co(II) + OOH^- \leftrightarrow Co(II) + {}^{\cdot}OOH$$

$$Co(II) + {}^{\cdot}OOH \leftrightarrow Co(II) + {}^{\cdot}O_2H$$

$$Co(II) + H_2O_2 \leftrightarrow Co(III) + {}^{\cdot}OH + OH^-$$

$${}^{\cdot}OH + {}^{\cdot}O_2H \leftrightarrow H_2O + O_2$$

For instance, an ultrasensitive sandwich-type electrochemical immunosensor based on platinum nanoparticles loaded-$Co_3O_4$/graphene nanosheets (Pt NPs/$Co_3O_4$/graphene) was employed as a label to quantitatively detect alpha-fetoprotein (AFP). It is worth mentioning that the prepared catalytic probe was not merely endowed with the advantages of each component but also exhibited better catalytic activity towards the reduction of $H_2O_2$. The peroxidase-like activity was increasingly improved with the ordinal incorporation of graphene, Pt NPs, and $Co_3O_4$. The cyclic voltammograms also proved the good catalytic properties of Pt NPs/$Co_3O_4$/graphene composites, which showed a dramatically increased reduction current after the addition of $H_2O_2$. With this incorporated signal amplification strategy, this electrochemical immunosensor exhibited a wide linear range from 0.1 pg $mL^{-1}$ to 60 ng $mL^{-1}$ and a low detection limit of 0.029 pg $mL^{-1}$ for AFP.[94]

Liao, Ma, and co-workers employed the reduced graphene oxide (rGO) as an excellent carrier, which was rich in oxygen-containing groups, to load with $Co_3O_4$ and mild dopamine-reduced silver nanoparticles (Ag NPs). With the self-polymerization of dopamine, the powerful properties and surface functional groups in polydopamine not only effectively reduced Ag NPs and promoted the amplification of electrochemical signals, but also protected the catalytic activity of $Co_3O_4$ and induced the double amplification of $H_2O_2$. For the construction of immunoprobes, the polymerization of dopamine maintains a lot of hydroxyl groups that can reduce silver ions to nanoparticle solids. Through a series of confirmatory experiments in Fig. 6A, a larger response current was obtained after the catalysis of rGO/$Co_3O_4$@PDA–Ag to $H_2O_2$ in comparison to other composites (rGO@PDA–Ag and rGO/$Co_3O_4$–Ag), which directly verified its good catalytic activity. Subsequent DPV curves in Fig. 6(B–D) also justified these results.[95]

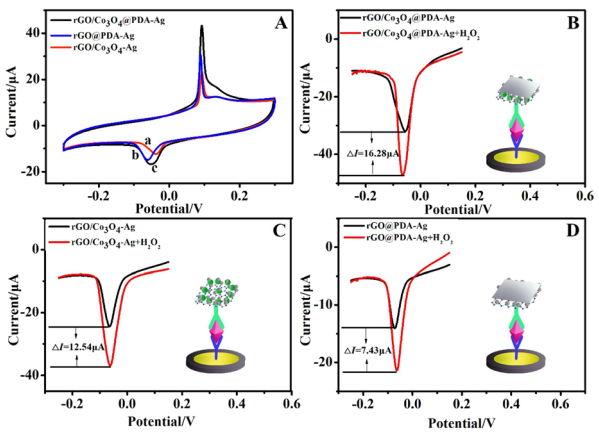


Fig. 6 (A) The cyclic voltammograms of rGO/$Co_3O_4$/Ag (a), rGO@PDA–Ag (b), and rGO/$Co_3O_4$@PDA–Ag (c) in 0.1 mol $L^{-1}$ PBS (pH = 7.0) containing 0.1 mol $L^{-1}$ KCl solution. (B–D) The differential pulse voltammograms of rGO/$Co_3O_4$@PDA–Ag, rGO/$Co_3O_4$–Ag and rGO@PDA–Ag in the presence or absence of $H_2O_2$ in 0.1 mol $L^{-1}$ PBS (pH = 7.0) containing 3 mmol $L^{-1}$ $H_2O_2$ and 0.1 mol $L^{-1}$ KCl solution. Reprinted with permission from ref. 95, copyright 2021 Elsevier.

There are many kinds of metal-based oxygenated compounds but they have the same poor conductivity as MOFs. They must undergo tedious pretreatment to functionalize their surface when they combine with biomolecules. In addition, they cannot exist stably in an acidic environment except when introduced as the metal source to release the desired ions in solution.

### 2.4 Prussian blue nanoparticles

For other iron-based nanozymes in electrochemical immunosensors, Prussian blue is an interesting example. The earliest study on Prussian blue on an electrode was reported by Neff in 1978 and involved the successful deposition of a thin layer on a platinum foil. Subsequently, Prussian blue was gradually exploited as a three-dimensional catalyst to replace horseradish peroxidase (HRP), which was ascribed to its zeolitic nature with a cubic unit cell of 10.2 Å and channel diameters of about 3.2 Å allowed the diffusion of low molecular weight molecules like $H_2O_2$.[96] In recent times, some relevant electrochemical immunosensors have also been proposed with Prussian blue being included in the preparation, modification, and application.[97–101] Wang and co-workers reported that a composite of Prussian blue nanocube-decorated molybdenum disulfide possessed excellent electrocatalytic ability toward $H_2O_2$ and was used in the design of a sensor for the label-free detection of carcinoembryonic antigen (CEA). Through the calculation of peak current changes in different medicated electrodes at 0.12 V, the $\Delta I$ of $MoS_2$–PBNCs/GCE was 8.36- and 11.78-fold higher than that of the $MoS_2$/GCE and PBNCs/GCE, respectively, resulting from the synergistic effect of $MoS_2$ and PBNCs. Moreover, they also had an ultra-low limit of detection of 0.54 pg $mL^{-1}$ for CEA.[102]

Our group has put forward a project for the *in situ* production of Prussian blue on the electrode surface with a sacrificial label for the detection of CA12-5. Assisted by the sacrificial label of ferric ion-polydopamine that can be quickly decomposed under the stimulation of acidic conditions, many Prussian blue nanoparticles with strong redox signals have been generated to form an electroactive immunosensing interface and further catalyse $H_2O_2$ to

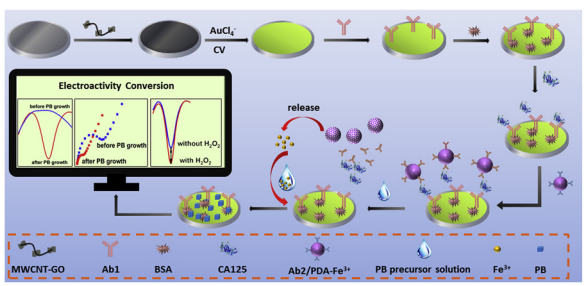


Fig. 7 Schematic diagram of the self-sacrificial label-assisted electroactivity conversion of the sensing interface for the ultrasensitive detection of CA12-5 (reprinted with permission from ref. 103, copyright 2019 Elsevier).

amplify the signal with the addition of precursor solution. This advanced immunoprobe paves the way for the production of peroxidase mimics, and self-annihilation eliminates its large hindrance effect (Fig. 7).[103]

For most PB-based electrochemical immunosensors, the major drawback is the lack of operational stability in alkaline solutions because the reduced form of PB, Prussian white, can be dissolved by hydroxide ions. Therefore, it is necessary to improve the stability of PB at relatively high pH and develop advanced methods that can effectively enhance the electrochemical stability of metal hexacyanoferrate.

### 2.5 Other transition metal-containing biomolecules

Besides the aforesaid Prussian blue, in some recent research studies, hemin peroxidase mimics have also been used in the catalysis of $H_2O_2$ for the amplification of electrochemical signals by accelerating electron transfer.[104–107] Enslaved to the poor aqueous solubility and high tendency to form inactive dimers, hemin, an iron porphyrin derivative, is always composited with other non-native supporters to avoid the decrease in peroxidase-like activity, such as carbon materials, MOFs, and some biomolecules. Yang *et al.* developed an alkaline phosphatase immunosensor based on a nanohybrid of platinum nanoparticles–porous ZnO spheres–hemin (Pt–pZnO–hemin) for the detection of influenza. Hemin with carboxylic functionality can be spontaneously adsorbed onto the Pt–ZnO surface with ester-like binding. A cascade reaction was immediately initiated once 1-naphthyl acid phosphate (p-NPP) was present in this system and 1-naphthol (1-NP) was subsequently formed on the electrode surface, further being oxidized to generate an electrochemical signal with the amplification of Pt–pZnO–hemin. On comparing Au–pZnO alone, Pt-pZnO and Au-pZnO-hemin, Pt-pZnO-hemin had higher catalytic ability profiting from the subsistence of hemin (Fig. 8).[108] Carbon materials like graphene, carbon spheres and carbon nanotubes also often serve as the matrix to immobilize hemin. To mitigate molecule aggregation and oxidative self-destruction, carbon sphere-loaded silver nanoparticles were inserted into hemin/reduce graphene oxide (hemin/rGO) as the spacer to overcome the irreversible stacking of rGO to prepare an immunoprobe. This mosaic structure helped hemin to expose more active sites to heighten the catalytic ability for $H_2O_2$ reduction. With this novel label, the electrochemical immunosensor for the detection of CEA presented an ultra-low LOD of 6.7 fg $mL^{-1}$.[109]

## Conclusions and perspectives

The development of peroxidase-active nanozymes is crucial for the wide application of electrochemical immunoassays as a means of tumor marker detection. There has been great interest in the introduction of peroxidase-active nanozyme systems as an effective strategy to enhance the analytical performance of electrochemical immunosensors. The

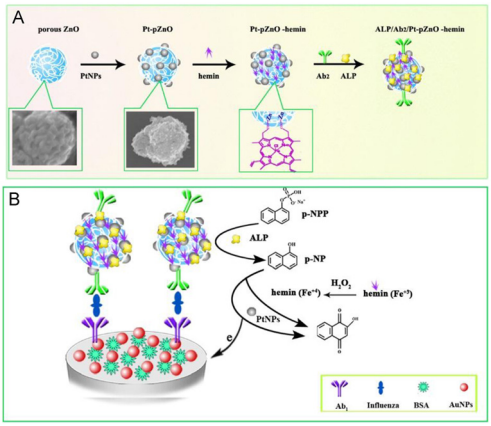


**Fig. 8** (A) The preparation of $Ab_2$ bioconjugates. (B) Schematic illustration of ALP and Pt–pZnO–hemin as the catalyst for the amplification signal (reprinted with permission from ref. 59, copyright 2019 Elsevier).

diversification of nanozyme compositions, high and tunable catalytic activity, ease of modification, large specific surface area, and low cost have resulted in their outstanding application prospects. This review has provided a detailed classification of peroxidase-active nanozymes and summarized its application in the design of immunosensing interfaces, which will give us a clear-cut understanding of how nanozymes affect such a colossal enhancement for the sensitivity, stability, and reproducibility of electrochemical immunosensors (Table 1). Conversely, although we have concluded that peroxidase-active nanozymes perform important roles in electrochemical immunosensors, there are still some problems to be solved in peroxidase-active nanozymes as follows: (1) although numerous nanomaterials have been proved as peroxidase mimics, the catalytic activities of most nanozymes are still much lower than those of the corresponding natural enzymes. (2) Besides, lots of peroxidase-like nanozymes generally have lower selectivity towards substrates and are often accompanied by other enzyme-like activities, like oxidase. One of the origins of this limitation is the lack of substrate-specific binding sites for the reaction substrates on the nanomaterial surface. (3) Representative peroxidase-active nanozymes like MOFs should have their conductivity and hydrophilicity in aqueous solution improved to meet the requirements of electrochemical biosensor applications. After all, these properties can directly influence electron transfer on the electrode surface. If these obstacles can be removed, the peroxidase-active nanozymes will be better applied in the design of electrochemical immunosensors, as well as the accurate detection of tumor markers.

## Author contributions

Jiejie Feng: investigation, writing – original draft. Tao Yao: investigation. Zhanfang Ma: funding acquisition, project administration, supervision.

**Table 1** Summary of the peroxidase-active nanozyme type, analyte, electrochemical method, detection range, and detection limit of the fabricated nanozyme-based electrochemical immunosensor

| Nanozyme | Biomarker | Method | Detection range | Detection limit | Year | Ref. |
|---|---|---|---|---|---|---|
| Pt/PdCu-3DGF | SCCA | *i–t* | 0.0001–1 ng $mL^{-1}$<br>1–30 ng $mL^{-1}$ | 25 fg $mL^{-1}$ | 2016 | 48 |
| Hemin@Fe-MIL-88$NH_2$/AuPt | Maduramicin | *i–t* | 0.1–50 ng $mL^{-1}$ | 0.045 ng $mL^{-1}$ | 2019 | 58 |
| N-GNRs-Fe-MOFs@Au NPs | Gal-3 | DPV | 0.0001–50 ng $mL^{-1}$ | 33.33 fg $mL^{-1}$ | 2018 | 59 |
| PdPt NDs@$NH_2$-MIL-53(Fe) | Prolactin | *i–t* | 0.001–500 ng $mL^{-1}$ | 1.15 pg $mL^{-1}$ | 2021 | 60 |
| GOx–Cu-MOFs | CA 15-3 | EIS | 0.01–10 mU $mL^{-1}$<br>0.01–100 U $mL^{-1}$ | 5.06 μU $mL^{-1}$ | 2019 | 64 |
| $Cu_2O$@Cu-MOF@Au NPs | CEA | *i–t* | 0.00005–80 ng $mL^{-1}$ | 17 fg $mL^{-1}$ | 2020 | 65 |
| Pd/$NH_2$-ZIF-67 | PSA | *i–t* | 0.0001–50 ng $mL^{-1}$ | 0.03 pg $mL^{-1}$ | 2019 | 75 |
| Co-BTC–GO-MOFs | $VEGF_{165}$ | DPV | $10^{-13}$–$10^{-6}$ M | 5.23 pM | 2020 | 76 |
| $Fe_3O_4$@$SiO_2$ | CEA | DPV | 0.001–80 ng $mL^{-1}$ | 0.2 pg $mL^{-1}$ | 2016 | 77 |
| Au–$Fe_3O_4$ | AFP | — | 0.01–40 ng $mL^{-1}$ | 2.3 pg $mL^{-1}$ | 2013 | 78 |
| $Fe(OH)_3$–NC | CA 19-9 | SWV | 0.00001–100 U $mL^{-1}$ | 0.785 μU $mL^{-1}$ | 2021 | 81 |
| $Cu_2O$@$TiO_2$–PtCu | Insulin | *i–t* | 0.0001–100 ng $mL^{-1}$ | 0.024 pg $mL^{-1}$ | 2019 | 85 |
| $Cu_2O_2$/ZIF-8 | CA 19-9 | SWV | 0.0001–100 U $mL^{-1}$ | 53.5 μU $mL^{-1}$ | 2020 | 86 |
| Pt NPs/$Co_3O_4$/graphene | AFP | *i–t* | 0.0001–60 ng $mL^{-1}$ | 0.029 pg $mL^{-1}$ | 2017 | 94 |
| rGO/$Co_3O_4$–Ag@PDA | CEA | DPV | 0.0005–80 ng $mL^{-1}$ | 0.17 pg $mL^{-1}$ | 2021 | 95 |
| $MoS_2$–PBNCs | CEA | DPV | 0.005–10 ng $mL^{-1}$ | 0.54 pg $mL^{-1}$ | 2017 | 102 |
| $Fe^{3+}$–PDA–PB | CA 12-5 | SWV | 0.00001–1000 U $mL^{-1}$ | 0.25 μU $mL^{-1}$ | 2019 | 103 |
| Pt–pZnO–hemin | Influenza | DPV | 0.001–60 ng $mL^{-1}$ | — | 2016 | 108 |
| Ag NPs@CS–hemin/rGO | CEA | *i–t* | 0.00002–200 ng $mL^{-1}$ | 6.7 fg $mL^{-1}$ | 2019 | 109 |

## Conflicts of interest

The authors declare no competing interests.

## Acknowledgements

The authors thank the funding of National Natural Science Foundation of China (22172104) and Joint Project of Beijing Municipal Education Commission and Beijing Natural Science Foundation (KZ202110028042).

## References

1 Z. X. Tang and Z. F. Ma, *Biosens. Bioelectron.*, 2017, **98**, 100–112.
2 W. Feng, X. Han, H. Hu, M. Chang, L. Ding, H. Xiang, Y. Chen and Y. Li, *Nat. Commun.*, 2021, **12**, 2203.
3 N. Zhang, X. T. Wang, Z. Xiong, L. Y. Huang, Y. Jin, A. J. Wang, P. X. Yuan, Y. B. He and J. J. Feng, *Anal. Chem.*, 2021, **93**, 17110–17118.
4 X. Y. Liang, J. C. Zhao and Z. F. Ma, *Sens. Actuators, B*, 2020, **304**, 127278.
5 T. Yao, J. J. Feng, Q. C. Xiong, C. S. Chu, Y. Xu, Z. F. Ma and H. Han, *Chem. Eng. J.*, 2022, **439**, 135599.
6 C. Zhao, X. Li, S. An, D. Zheng, S. Pei, X. Zheng, Y. Liu, Q. Yao, M. Yang and L. Dai, *Sci. Bull.*, 2019, **64**, 1272–1279.
7 J. C. Zhao and Z. F. Ma, *Biosens. Bioelectron.*, 2018, **102**, 316–320.
8 Z. Zhang, T. Yao, H. L. Han and Z. F. Ma, *Anal. Chem.*, 2022, **94**, 16231–16236.
9 Z. Li, J. Zhang, Y. Huang, J. Zhai, G. Liao, Z. Wang and C. Ning, *Coord. Chem. Rev.*, 2022, **471**, 214723.
10 D. S. Zhang, W. X. Li, H. Q. Wang and Z. F. Ma, *Sens. Actuators, B*, 2018, **258**, 141–147.
11 P. Nandhakumar, G. Kim, S. Park, S. Kim, S. Kim, J. K. Park, N.-S. Lee, Y. H. Yoon and H. Yang, *Angew. Chem., Int. Ed.*, 2020, **59**, 22419–22422.
12 Z. Farka, T. Jurik, D. Kovar, L. Trnkova and P. Skladal, *Chem. Rev.*, 2017, **117**, 9973–10042.
13 R. Liu, P. Wu, L. Yang, X. Hou and Y. Lv, *Mass Spectrom. Rev.*, 2014, **33**, 373–393.
14 G. Mao, S. Ye, W. Yin, Y. Yang, X. Ji, J. He, Y. Liu, J. Dai, Z. He and Y. Ma, *Nano Res.*, 2023, **16**, 2859–2865.
15 Y. Wang, G. Zhao, H. Chi, S. Yang, Q. Niu, D. Wu, W. Cao, T. Li, H. Ma and Q. Wei, *J. Am. Chem. Soc.*, 2021, **143**, 504–512.
16 L. H. Zhao, H. L. Han and Z. F. Ma, *Biosens. Bioelectron.*, 2018, **101**, 304–310.
17 J. J. Feng, H. Q. Wang and Z. F. Ma, *Microchim. Acta*, 2020, **187**, 95.
18 Y. Chen, A. J. Wang, P. X. Yuan, X. Luo, Y. Xue and J. J. Feng, *Biosens. Bioelectron.*, 2019, **132**, 294–301.
19 Y. W. Mao, J. X. Zhang, D. N. Chen, A. J. Wang and J. J. Feng, *Sens. Actuators, B*, 2022, **370**, 132416.
20 Y. G. Feng, J. W. He, L. Y. Jiang, D. N. Chen, A. J. Wang and J. J. Feng, *Sens. Actuators, B*, 2022, **358**, 131518.
21 J. J. Feng, C. S. Chu and Z. F. Ma, *Electrochem. Commun.*, 2021, **125**, 106970.
22 N. Wongkaew, M. Simsek, C. Griesche and A. J. Baeumner, *Chem. Rev.*, 2019, **119**, 120–194.
23 Y. Xu, F. Wang, Y. Zheng, J. J. Feng, Z. Zhang, H. L. Han and Z. F. Ma, *Sens. Actuators, B*, 2022, **372**, 132625.
24 J. J. Feng, X. Y. Liang and Z. F. Ma, *Biosens. Bioelectron.*, 2021, **175**, 112853.
25 Q. Wang, H. Wei, Z. Zhang, E. Wang and S. Dong, *TrAC, Trends Anal. Chem.*, 2018, **105**, 218–224.
26 B. B. Kou, Y. Q. Chai, Y. L. Yuan and R. Yuan, *Chem. Sci.*, 2021, **12**, 407–411.

27 B. Liu, Y. Wang, Y. Chen, L. Guo and G. Wei, *J. Mater. Chem. B*, 2020, **8**, 10065.
28 Y. Huang, J. Ren and X. Qu, *Chem. Rev.*, 2019, **119**, 4357–4412.
29 Y. Zhao, X. Xiao, M. Zou, B. Ding, H. Xiao, M. Wang, F. Jiang, Z. Cheng, P. A. Ma and J. Lin, *Adv. Mater.*, 2020, **33**, 2006363.
30 Z. Wang, R. Zhang, X. Yan and K. Fan, *Mater. Today*, 2020, **41**, 81–119.
31 M. K. Masud, S. Yadav, M. N. Islam, N. T. Nguyen, C. Salomon, R. Kline, H. R. Alamri, Z. A. Alothman, Y. Yamauchi, M. S. A. Hossain and M. J. A. Shiddiky, *Anal. Chem.*, 2017, **89**, 11005–11013.
32 D. Wang, D. Jana and Y. Zhao, *Acc. Chem. Res.*, 2020, **53**, 1389–1400.
33 S. Yin and Z. F. Ma, *Sens. Actuators, B*, 2019, **281**, 857–863.
34 Y. Ai, Z. N. Hu, X. Liang, H. B. Sun, H. Xin and Q. Liang, *Adv. Funct. Mater.*, 2021, **32**, 2110432.
35 N. N. Zhang, Y. Xu and Z. F. Ma, *Sens. Actuators, B*, 2020, **317**, 128244.
36 L. Y. Hu, L. X. Chen, M. T. Liu, A. J. Wang, L. J. Wu and J. J. Feng, *J. Colloid Interface Sci.*, 2017, **493**, 94–102.
37 R. G. Mahmudunnabi, F. Z. Farhana, N. Kashaninejad, S. H. Firoz, Y.-B. Shim and M. J. A. Shiddiky, *Analyst*, 2020, **145**, 4398–4420.
38 Y. Lin, J. Ren and X. Qu, *Adv. Mater.*, 2014, **26**, 4200–4217.
39 C. Zhang and Z. F. Ma, *Biosens. Bioelectron.*, 2019, **143**, 111612.
40 W. X. Li, Q. F. Rong and Z. F. Ma, *New J. Chem.*, 2017, **41**, 1124.
41 J. Shan and Z. F. Ma, *Microchim. Acta*, 2017, **184**, 969–979.
42 X. Pei, B. Zhang, J. Tang, B. Liu, W. Lai and D. Tang, *Anal. Chim. Acta*, 2013, **758**, 1–18.
43 X. Zhang, Y. Li, H. Lv, Z. Gao, C. Zhang, S. Zhang, Y. Wang, Z. Xu and Z. Zhao, *J. Electrochem. Soc.*, 2018, **165**, B931–B938.
44 M. J. Ahemad, D.-S. Kim, T. Duc Le, L. R. Nagappagari, G.-J. Oh, G.-S. Shin, U. Ahmad, S. A. Akbar and Y. T. Yu, *ACS Appl. Nano Mater.*, 2022, **5**, 18568–18580.
45 C. He, M. Asif, Q. Liu, F. Xiao, H. Liu and B. Y. Xia, *Adv. Mater. Technol.*, 2022, **8**, 2200272.
46 R. R. A. Soares, R. G. Hjort, C. C. Pola, K. Parate, E. L. Reis, N. F. F. Soares, E. S. McLamore, J. C. Claussen and C. L. Gomes, *ACS Sens.*, 2020, **5**, 1900–1911.
47 L. Ji, Z. Guo, T. Yan, H. Ma, B. Du, Y. Li and Q. Wei, *Biosens. Bioelectron.*, 2015, **68**, 757–762.
48 Y. Liu, H. Ma, J. Gao, D. Wu, X. Ren, T. Yan, X. Pang and Q. Wei, *Biosens. Bioelectron.*, 2016, **79**, 71–78.
49 X. Fu, B. Ding and D. D'Alessandro, *Coord. Chem. Rev.*, 2023, **475**, 214814.
50 S. Biswas, Q. Lan, C. Li and X. H. Xia, *Anal. Chem.*, 2022, **94**, 3013–3019.
51 X. Qin, B. Wang, X. Li, Y. Ding, X. Yang, Y. Zhou, W. Xu, M. Xu and C. Gu, *J. Electroanal. Chem.*, 2022, **911**, 116186.
52 S. Palanisamy, D. Senthil Raja, B. Subramani, T. H. Wu and Y. M. Wang, *ACS Appl. Mater. Interfaces*, 2020, **12**, 32468–32476.
53 W.-T. Li, S.-Y. Dong, H. Chen, Y.-Q. An, J. Zhang, L.-Y. Wang and J.-J. Zhu, *Chem. Eng. J.*, 2022, **446**, 136850.
54 M. Lian, Y. Shi, L. Chen, Y. Qin, W. Zhang, J. Zhao and D. Chen, *ACS Sens.*, 2022, **7**, 2701–2709.
55 W. Xu, W. Xue, H. Huang, J. Wang, C. Zhong and D. Mei, *Appl. Catal., B*, 2021, **291**, 120129.
56 C. Du, Y. Zhang, Z. Zhang, L. Zhou, G. Yu, X. Wen, T. Chi, G. Wang, Y. Su, F. Deng, Y. Lv and H. Zhu, *Chem. Eng. J.*, 2022, **431**, 133932.
57 P. Xiao, G. Zhu, X. Shang, B. Hu, B. Zhang, Z. Tang, J. Yang and J. Liu, *J. Electroanal. Chem.*, 2022, **916**, 116382.
58 M. Hu, Y. Wang, J. Yang, Y. Sun, G. Xing, R. Deng, X. Hu and G. Zhang, *Biosens. Bioelectron.*, 2019, **142**, 111554.
59 Z. Tang, J. He, J. Chen, Y. Niu, Y. Zhao, Y. Zhang and C. Yu, *Biosens. Bioelectron.*, 2018, **101**, 253–259.
60 F. Zhang, F. Huang, W. Gong, F. Tian, H. Wu, S. Ding, S. Li and R. Luo, *J. Electroanal. Chem.*, 2021, **882**, 115032.
61 M. Rezki, N. L. W. Septiani, M. Iqbal, S. Harimurti, P. Sambegoro, D. R. Adhika and B. Yuliarto, *J. Mater. Chem. B*, 2021, **9**, 5711–5721.
62 M. L. Yola, *Microchim. Acta*, 2021, **188**, 78.
63 H. Liang, C. Chen, J. Zeng, M. Zhou, L. Wang, G. Ning, Q. Duan, R. Han, H. Liu, H. Zhao and C.-P. Li, *ACS Appl. Nano Mater.*, 2022, **5**, 16774–16783.
64 C. Zhang, D. S. Zhang, Z. F. Ma and H. L. Han, *Biosens. Bioelectron.*, 2019, **137**, 1–7.
65 W. J. Li, Y. Yang, C. Y. Ma, Y. J. Song, C. L. Hong and X. W. Qiao, *J. Mater. Sci.*, 2020, **55**, 13980–13994.
66 Y. Song, M. Xu, Z. Li, L. He, M. Hu, L. He, Z. Zhang and M. Du, *Sens. Actuators, B*, 2020, **311**, 127927.
67 M. Wang, Z. Shen, X. Zhao, F. Duanmu, H. Yu and H. Ji, *J. Hazard. Mater.*, 2019, **371**, 352–361.
68 J. Zhou, Q. Yang, Q. Xie, H. Ou, X. Lin, A. Zeb, L. Hu, Y. Wu and G. Ma, *J. Mater. Sci. Technol.*, 2022, **96**, 262–284.
69 W. K. Fan and M. Tahir, *Energy Convers. Manage.*, 2022, **253**, 115180.
70 N. Bagheri, B. Habibi, A. Khataee and J. Hassanzadeh, *Talanta*, 2019, **201**, 286–294.
71 L. Cao, J. Cai, W. Deng, Y. Tan and Q. Xie, *Anal. Chem.*, 2020, **92**, 16267–16273.
72 X. Li, Y. Du, H. Wang, H. Ma, D. Wu, X. Ren, Q. Wei and J. J. Xu, *Anal. Chem.*, 2020, **92**, 12693–12699.
73 S. Wang, Y. Zhao, M. Wang, H. Li, M. Saqib, C. Ge, X. Zhang and Y. Jin, *Anal. Chem.*, 2019, **91**, 3048–3054.
74 X. Shi, Y. Xie, L. Chen, J. Lu, L. Zhang and D. Sun, *Bioelectrochemistry*, 2023, **149**, 108278.
75 L. Dai, Y. Li, Y. Wang, X. Luo, D. Wei, R. Feng, T. Yan, X. Ren, B. Du and Q. Wei, *Biosens. Bioelectron.*, 2019, **132**, 97–104.
76 S. Singh, A. Numan, Y. Zhan, V. Singh, A. Alam, T. Van Hung and N. D. Nam, *RSC Adv.*, 2020, **10**, 27288–27296.
77 T. Feng, X. Qiao, H. Wang, Z. Sun and C. Hong, *Biosens. Bioelectron.*, 2016, **79**, 48–54.
78 G. K. Parshetti, F.-H. Lin and R.-A. Doong, *Sens. Actuators, B*, 2013, **186**, 34–43.

79 R. Bhattacharjee, S. Tanaka, S. Moriam, M. K. Masud, J. Lin, S. M. Alshehri, T. Ahamad, R. R. Salunkhe, N. T. Nguyen, Y. Yamauchi, M. S. A. Hossain and M. J. A. Shiddiky, *J. Mater. Chem. B*, 2018, **6**, 4783–4791.
80 S. Yadav, M. K. Masud, M. N. Islam, V. Gopalan, A. K. Lam, S. Tanaka, N. T. Nguyen, M. S. A. Hossain, C. Li, Y. Yamauchi and M. J. A. Shiddiky, *Nanoscale*, 2017, **9**, 8805–8814.
81 X. Z. Meng, Y. Xu, N. N. Zhang, B. C. Ma, Z. F. Ma and H. L. Han, *Sens. Actuators, B*, 2021, **338**, 129840.
82 T. Wang, X. C. Yang, Y. Ding, Y. J. Zhang, Y. Q. Ru, J. J. Tan, F. Xu, W. W. Gao and Y. M. Xia, *J. Mater. Chem. B*, 2023, **11**, 1760–1772.
83 J. C. Munyemana, J. Chen, X. Wei, M. C. Ali, Y. Han and H. Qiu, *Anal. Bioanal. Chem.*, 2020, **412**, 4629–4638.
84 L. Zhao, D. Si, Y. Zhao, L. Wang, H. An, H. Ye, Q. Xin and Y. Zhang, *Colloids Surf., A*, 2022, **644**, 128876.
85 F. Li, J. Feng, Z. Gao, L. Shi, D. Wu, B. Du and Q. Wei, *ACS Appl. Mater. Interfaces*, 2019, **11**, 8945–8953.
86 H. Q. Wang and Z. F. Ma, *Biosens. Bioelectron.*, 2020, **169**, 112644.
87 J. Bae, D. Shin, H. Jeong, B.-S. Kim, J. W. Han and H. Lee, *ACS Catal.*, 2019, **9**, 10093–10100.
88 Y. Li, F.-M. Li, X.-Y. Meng, S.-N. Li, J.-H. Zeng and Y. Chen, *ACS Catal.*, 2018, **8**, 1913–1920.
89 T. Zhou, P. Lu, Z. Zhang, Q. Wang and A. Umar, *Sens. Actuators, B*, 2016, **235**, 457–465.
90 X. Liu, Y. Du, S. Wang, Y. Huang, Y. Tian, D. Garcia-Lojo, I. Perez-Juste, J. Perez-Juste, I. Pastoriza-Santos and G. Zheng, *Small*, 2023, e2205187.
91 L. Bao, T. Li, S. Chen, C. Peng, L. Li, Q. Xu, Y. Chen, E. Ou and W. Xu, *Small*, 2017, **13**, 1602077.
92 W. Yang, X. Yang, L. Zhu, H. Chu, X. Li and W. Xu, *Coord. Chem. Rev.*, 2021, **448**, 214170.
93 A. Rokicińska, M. Drozdek, E. Bogdan, A. Węgrzynowicz, P. Michorczyk and P. Kuśtrowski, *Catal. Today*, 2021, **375**, 369–376.
94 L. Liu, L. Tian, G. Zhao, Y. Huang, Q. Wei and W. Cao, *Anal. Chim. Acta*, 2017, **986**, 138–144.
95 X. Liao, C. Ma, C. Zhao, W. Li, Y. Song, C. Hong and X. Qiao, *Microchem. J.*, 2021, **160**, 105602.
96 F. Ricci and G. Palleschi, *Biosens. Bioelectron.*, 2005, **21**, 389–407.
97 J. Li, X. Yan, X. Li, X. Zhang and J. Chen, *Talanta*, 2018, **179**, 726–733.
98 M. Wang, M. Jiang, P. Li, M. Yuan, C. Zhao, W. Lai, J. Li, C. Hong and Y. Qi, *Anal. Chim. Acta*, 2023, **1257**, 341143.
99 G. Wang, G. Zhang, H. Huang and L. Wang, *Chin. J. Chem.*, 2012, **30**, 485–490.
100 Z. Yuan, H. Dai, X. Liu, S. Duan, Y. Shen, Q. Zhang, Z. Shu, A. Xiao and J. Wang, *Food Chem.*, 2023, **405**, 134842.
101 M. M. Habibi, S. A. Mirhosseini, S. Sajjadi and A. H. Keihan, *Bioelectrochemistry*, 2021, **142**, 107887.
102 S. Su, X. Han, Z. Lu, W. Liu, D. Zhu, J. Chao, C. Fan, L. Wang, S. Song, L. Weng and L. Wang, *ACS Appl. Mater. Interfaces*, 2017, **9**, 12773–12781.
103 S. Yin and Z. F. Ma, *Biosens. Bioelectron.*, 2019, **140**, 111355.
104 C. Zhang, S. Zhang, Y. Jia, Y. Li, P. Wang, Q. Liu, Z. Xu, X. Li and Y. Dong, *Biosens. Bioelectron.*, 2019, **126**, 785–791.
105 X. Li, J. Li, C. Zhu, X. Zhang and J. Chen, *Talanta*, 2018, **182**, 292–298.
106 Y.-C. Zhou, M. Zhao, Y.-Q. Yu, Y.-M. Lei, Y.-Q. Chai, R. Yuan and Y. Zhuo, *Sens. Actuators, B*, 2017, **246**, 1–8.
107 Q. Wang, Y. Song, H. Xie, Y. Chai, Y. Yuan and R. Yuan, *Chem. Commun.*, 2015, **51**, 1255–1258.
108 Z. H. Yang, Y. Zhuo, R. Yuan and Y. Q. Chai, *Biosens. Bioelectron.*, 2016, **78**, 321–327.
109 C. Zhang, S. Zhang, Y. Jia, Y. Li, P. Wang, Q. Liu, Z. Xu, X. Li and Y. Dong, *Biosens. Bioelectron.*, 2019, **126**, 785–791.
110 M. K. Masud, J. Kim, M. M. Billah, K. Wood, M. J. A. Shiddiky, N. T. Nguyen, R. K. Parsapur, Y. V. Kaneti, A. A. Alshehri, Y. G. Alghamidi, K. A. Alzahrani, M. Adharvanachari, P. Selvam, M. S. A. Hossain and Y. Yamauchi, *J. Mater. Chem. B*, 2019, **7**, 5412–5422.
111 S. Tanaka, M. K. Masud, Y. V. Kaneti, M. J. A. Shiddiky, A. Fatehmulla, A. M. Aldhafiri, W. A. Farooq, Y. Bando, M. S. A. Hossain and Y. Yamauchi, *ChemNanoMat*, 2019, **5**, 506–513.
112 M. A. Wahab, S. M. A. Hossain, M. K. Masud, H. Park, A. Ashok, M. Mustapić, M. Kim, D. Patel, M. Shahbazi, M. S. A. Hossain, Y. Yamauchi and Y. V. Kaneti, *Sens. Actuators, B*, 2022, **366**, 131980.